

Effect of Chemically synthesis compared to biosynthesized zinc oxide nanoparticles using extract of *Vitex agnus* on the expression of MexAB-OprM efflux pump genes of Multi-Drug Resistance *Pseudomonas aeruginosa*

Shams Al-Shomos Khalis Khames  , Shatha Thanoon Ahmed*  

Department of Biology, College of Science for Women, University of Baghdad, Baghdad, Iraq.

*Corresponding Author.

Received 17/02/2024, Revised 31/05/2024, Accepted 02/04/2024, Published Online First 20/06/2024,
Published 22/12/2024



© 2022 The Author(s). Published by College of Science for Women, University of Baghdad.

This is an open-access article distributed under the terms of the [Creative Commons Attribution 4.0 International License](https://creativecommons.org/licenses/by/4.0/), which permits unrestricted use, distribution, and reproduction in any medium, provided the original work is properly cited.

Abstract

The current study's goal was to find out how the expression of the efflux pump genes (MexAB-OprM) in MDR *P. aeruginosa* isolates was influenced by chemically manufactured Zinc Oxide Nanoparticles using sol-gel method as compared to biosynthesized Zinc Oxide Nanoparticles using *Vitex agnus-castus* leaves extract. PCR analysis was used to confirm the presence of 16S rRNA gene in all 16 *P. aeruginosa* isolates. The findings indicated that *P. aeruginosa* tested positive for 16S rRNA (100%), and 7 (43.75%) of the isolates were MDR. All MDR isolates carried MexA, MexB and OprM genes. The *Vitex* extract's GC-MS analysis exposed the existence of active chemicals. The size of the synthesized Zinc Oxide Nanoparticles ranged from 22 to 74 nm. The Minimum inhibitory concentration values for chemically synthesized NPs, biosynthesized NPs, and *Vitex* extract against concentrations were 1024, 256, and 512 µg/mL, respectively, when tested against MDR isolates. Biosynthesized Zinc Oxide Nanoparticles have a greater inhibitory effect on efflux pump genes than chemically synthesized Zinc Oxide Nanoparticles and *Vitex* extract in the expression of MexA, MexB, and OprM genes in samples treated with sub MIC of Zinc Oxide Nanoparticles and plant extract compared to non-treated samples. One way that nanoparticles work against bacteria is by suppressing the expression of the efflux pump genes, which lowers the number of active efflux pumps on the cell surface. As a result, Zinc Oxide Nanoparticles are regarded by the pharmaceutical sector as a potential medicinal option.

Keywords: *Pseudomonas aeruginosa*, ZnO NPs, *Vitex*, MexA, MexB, OprM.

Introduction

Pseudomonas aeruginosa (*P. aeruginosa*) is a broadly spread opportunistic bacteria that is linked to healthcare-associated diseases and can cause serious contagions in plants, animals, and mammals^{1,2}. Multidrug-resistant strains' (MDR) appearance is perceived as a serious public health concern³. There

are several virulence mechanisms through which the bacteria have grown⁴. Among them, the overexpression of efflux pump systems is the main mechanism leading to multidrug resistance (MDR)⁵. Antibiotics only experience sub-inhibitory levels in bacteria as a result of efflux pumps, which can

lower intracellular drug concentrations and prevent antibiotics from reaching their targets in microbial cells. This could lead to other resistance mechanisms, such as changes in the structure of antibiotic targets as a result of mutation or enzymatic deactivation of antibiotics⁶. Efflux pumps have three resistance settings. First, they induce intrinsic resistance in the bacteria by expressing at the basic level. Second, mutant bacteria acquire resistance as a result of pump overexpression. Third, transient overexpression of pumps would result in resistance in strains that proliferate under stress⁷. There are six distinct multidrug efflux mechanisms in *P. aeruginosa*: Finding alternatives to antibiotics is instantly required because *MexAB-OprM*, the majority-studied pump of this bacterium, has the widest spectrum of substrates among all bacterial effluxes, including quinolones, tetracycline, chloramphenicol, trimethoprim, β -lactam, β -lactamase inhibitors, macrolides, azithromycin, colistin, detergents, and dyes⁸. Drug-resistant patients may benefit significantly from the use of nanoparticles as a therapeutic alternative in the future⁹. One such material is zinc oxide nanoparticles or ZnO-NPs. Zinc oxide nanoparticles with great biocompatibility, low toxicity, and affordability are utilized in biological applications. In biomedicine, ZnO NPs have shown great potential, especially in the areas of antibacterial and cancer treatment¹⁰. ZnO NPs were produced via chemical, biological, and physical processes¹¹. The biological method is an effective process that substitutes expensive and harmful chemicals with

natural compounds (such as plant extracts and microorganisms) that are used as capping, stabilizing, and reducing agents. Physical and chemical methods, on the other hand, are more costly and require a lot of labor and time in addition to creating a lot of secondary waste from the chemical agents used for the reduction and precipitation¹². Compared to the others, the plant-based green synthesis process is used more frequently. Compared to the fungal and bacteria-mediated syntheses, the plants are safer for biological systems and easier to locate. Additionally, because plant extracts contain active substances such as terpenoids, alkaloids, phenols, tannins, and vitamins, they are well-known for their usage in medicine and the environment¹³. The Verbenaceae plant *Vitex agnus-castus*, often known as the chasteberry or chaste tree, is native to the Mediterranean region as well as Asia, Europe, and North America. This herb has been utilized for traditional medicinal reasons to treat gynecological disorders for over 2500 years¹⁴. Furthermore, a multitude of bioactive metabolites (such as flavonoids, ketosteroids, iridoids, essential oils, etc.) found in *Vitex agnus-castus* exhibit outstanding activity in the environmentally friendly synthesis of ZnO nanoparticles with potent reducing qualities¹⁵. The current work aimed to explore the influence on the expression level of the efflux pump genes (*MexAB-OprM*) in MDR-*P. aeruginosa* by comparing the biosynthesized ZnO NPs using leaves extract of *V. agnus-castus* to chemically synthesized ZnO NPs as well as alcoholic extract of *V. agnus* leaves.

Materials and Methods

P. aeruginosa isolates and molecular identification

This investigation was conducted on sixteen *P. aeruginosa* isolates from various illnesses that were collected over five months (October 2022–February 2023) from Al Kindy Teaching Hospital in Baghdad. After being incubated at 37°C for 24 hours, cetrinide agar, a selective medium for *P. aeruginosa* isolation, was used to screen all 16 isolates. The results were then authenticated by PCR using particular primer pairs for the 16S rRNA

gene of *P. aeruginosa* (Table 1). Genomic DNA was isolated following the Wizard genomic DNA purification kit/Promega manufacturer's instructions. PCR was used to find the 16S rRNA gene using a particular primer, as indicated in table 1. The following protocol was carried out using an Eppendorf, Germany-based Mastercycler/nexus-PCR Thermal Cycler: First, denaturation was done for two minutes at 95 °C. Thereafter, denaturation was done for 35 cycles at 94 °C for 20 seconds, annealing for 20 seconds at 58 °C, and elongation for 40 seconds at 72 °C. Finally, one cycle at 72 °C

for five minutes was conducted. Following an hour of 70-volt electrophoresis on 1.5% agarose gel, the amplified products were stained with ethidium bromide.

Antibiotics susceptibility test

The following six antibiotic classes' susceptibility tests were conducted using the Kirby-Bauer method (1968) on Muller-Hinton agar (Bio lab, Hungary) and described by clinical laboratories standard specified CLSI (2023) which are used for treatment of *P. aeruginosa*. 1. Aminoglycoside (30 µg Gentamicin and 10 µg Amikacin) 2. Carbapenem (10 µg each of Meropenem and Imipenem) 3. Levofloxacin (5 µg) and Ciprofloxacin (5 µg) fluoroquinolones 4. Ceftazidime (30 µg) via Cephalosporin 5. Monobactam (30 µg Aztreonam) and 6. Beta-lactamase inhibitor (100 ug Piperacillin,

100/10 µg Piperacillin-Tazobactam, and 75/10 µg Ticarcillin-Clavulanate).

Detection *P. aeruginosa* efflux pump genes

Using uniplex PCR, four multidrug-resistant bacterial isolates were chosen for the current search to detect the existence of efflux pump genes (*MexA*, *MexB*, and *OprM*) connected to a housekeeping gene (*rpsL*). A 25 µl final volume was used for PCR. 12.5 µl of Amplicon, Denmark's Master mix, 1.5 µl (10pmol/µl) of each primer (provided by Bioneer Co., Korea), 4 µl of template DNA, and 5.5 µl of sterile deionized distilled water were used in this reaction. Tables 1 and 2 include the primer sequence and conditions needed to duplicate these genes. Using a 1 kb DNA ladder (Roche, Germany), the PCR products were electrophoresed on 2% agarose containing 0.5 mg/mL of ethidium bromide for 60 minutes at 70 volts.

Table 1. Primer's sequence used in the present study.

Primer	Primer sequence (5'→3')	Product size (bp)	Tm	Reference
<i>MexA</i>				
Forward	TGACCCTGAATACCGAGCTG	168	60	Designed
Reverse	GGTAGTCGGCCTCGTAGGT		59	
<i>MexB</i>				
Forward	AGGTCCAGGTGCAGAACAAG	158	60	Designed
Reverse	GTTCGACAGGTCTTCCTTGG		59	
<i>OprM</i>				
Forward	CCATGAGCCGCCAACTGTC	180	58	16
Reverse	CCTGGAACGCCGTCTGGAT		59	
<i>rpsL</i>				
Forward	GCAAGCGCATGGTCGACAAGA	201	59	17
Reverse	CGCTGTGCTCTTGCAGGTTGTGA		60	
<i>16SrRNA</i>				
Forward	GGGGGATCTTCGGACCTCA	956	58	18
Reverse	TCCTTAGAGTGCCCACCCG		59	

Table 2. Conditions of PCR program.

Stages	Temperature (°C)	Period	Cycles number
Initial denaturation	94	5 minutes	1
Denaturation	94	30 seconds	
Annealing	55* , 57**	30 seconds	35
Elongation	72	20 seconds	
Final elongation	72	7 minutes	1

Note.**MexA*, *MexB*, *OprM* ***rpsL*

Preparation and Characterization of *V. agnus-castus* extract and synthesized ZnO-NPs

The botanical herbarium at the University of Baghdad/ College of Science for Women verified the species identity of the *V. agnus* leaves, which were purchased from AL-Jadriya gardens in Baghdad. To get rid of the dust particles on the surface, fresh *V. agnus* leaves have been repeatedly cleaned with distilled water. With minor adjustments, the method for extracting *Vitex* leaves was created as described by ¹⁹. The soxhlet system was used, and hexane and methanol were used as solvents, respectively. A firmly closed funnel-shaped filter paper was filled with 100 gm. of leaf powder, and the filter paper was then located in the soxhlet system. 500 ml of solvent was added and allowed to sit for 24 hours at room temperature. To obtain a dark brown crude extract, the extract was focused using a rotary evaporator with a water bath set at 40°C. Up until it was used, the crude extract was stored in a sterile container at 4°C. Additionally, an alcoholic *Vitex* leaf extract was made to use a gas chromatography-integrated mass spectrometer (GC-MS) apparatus to identify the active components.

Synthesis of ZnONPs

The main phases of the experiment were preparing ZnO-NPs using two different methods: biosynthesis, as described by ²⁰ with certain modifications, and chemical synthesis using the sol-gel approach, as described by ²¹. After heating 100 ml of *Vitex* extract to 60°C using a magnetic stirrer, 10 gm. of zinc nitrate Zn(NO₃)₂ was added. It is cooked until a creamy white paste forms. Subsequently, the dough is cleaned with distilled water and baked for two hours at 400 °C. Next, ZnONPs filled with active ingredients from the *Vitex* extract will produce a white powder. Using an X-ray diffractometer, the produced ZnO-NPs were subjected to an X-ray diffraction (XRD) test to evaluate the crystal structure of the particles and estimate their size ²². Additionally, to employing scanning electron microscopy (SEM) to ascertain the phenotypic and structural properties of particles ²³.

Antibacterial activity of ZnO-NPs and *Vitex* extract, Minimum Inhibitory Concentration (MIC) determination

The Minimum Inhibitory Concentration (MIC) was defined as the lowest concentration at which the color remained unaltered. Following ²⁴, the MIC was completed. To achieve a concentration, range from 8 to 8192 µg/ml, a stock solution (10000 µg/m) of each chemically manufactured ZnO NPs, biosynthesized ZnO NPs, and *Vitex* extract were serially diluted in 96-well microtiter plates using Mueller Hinton broth. Each bacterial culture (1.5 ×10⁸ CFU/ml) was prepared overnight, and 10 µl of the culture was added to each well. For 24 hours, a microtiter plate was incubated at 37°C. Subsequently, each well received 5 µl (6.75 mg/ml) of resazurin dye (Thermo Fisher, USA), and they were incubated for an additional 4 hours at 37°C. The color transition from purple to pink was inspected.

Gene Expression of the Efflux Pump genes using qRT-PCR

For four MDR *P. aeruginosa* isolates, the gene expression of efflux pumps was assessed using the quantitative Real-Time PCR technique both before and after each isolate was treated with chemically produced ZnONPs, biosynthesized ZnO NPs, and *Vitex* extract at sub-MIC.

RNA extraction

Four sterile microcentrifuge tubes with three milliliters of nutritive broth were inoculated with one milliliter of the bacterial inoculum suspension made from fresh cultures of each *P. aeruginosa* isolate. Three of these tubes were treated with one milliliter of sub MIC of each chem.ZnO NPS, bioZnO NPS, and *Vitex* extract; the fourth tube served as a control (not treated). All tubes were incubated for 18–24 hours at 37°C. The TransGen, Biotech, China TransZol up plus RNA Kit was used to extract RNA following the manufacturer's instructions. In the event of material shortage, RNA was additionally extracted for every isolate of *P. aeruginosa* (gene expression control). RNA concentration and purity were assessed for the extracted RNA quantity using Nanodrop (Quawell, China).

RT-qPCR reaction and program:

Reverse transcription was carried out using the GoTaq®1-Step RT-qPCR kit, and then the efflux pump genes (*MexA*, *MexB*, and *OprM*) were amplified using quantitative real-time PCR. Following the manufacturer's recommendations, a 20µl volume reaction was used for the operation. The materials needed were 10µl of qPCR Master Mix 2X, 1µl each of the forward and reverse

primers, 0.5µl of each GoScript RT Mix and MgCl₂, 3µl water, and 4µl of the extracted RNA for reverse transcription. Using the primers listed in Table 1, an RT-PCR thermal cycler was used, and the relative expression values of the efflux pump genes were compared to *rpsL*, a housekeeping gene. The RT-qPCR procedure is displayed in Table 3. Using the $2^{-\Delta C_t}$ technique, the relative gene expression levels in treated and untreated isolates were compared.

Table 3. Conditions of RT-qPCR program.

Stage	Temperature (°C)	Period	Cycle
Reverse transcription	37	15 min.	1
Reverse transcriptase inactivation and GoTaq® DNA Polymerase activation	95	10 min.	1
Denaturation	95	30 sec.	40
Annealing	55* 57**	30 sec.	
Elongation	72	30 sec.	

Note. * *MexA*, *MexB* and *OprM*; ***rpsL*

Statistical Analysis

The Statistical Analysis System- SAS (2018) program was utilized to ascertain the impact of different variables on the study parameters. To compare means significantly, the Least Significant

Difference (LSD) test Analysis of Variation (ANOVA) was employed. A significant comparison between percentages (0.05 and 0.01 probability) was made using the Chi-square test. An estimate of the correlation coefficient between variables was conducted in this study.

Results and Discussion

Molecular identification of isolates

Sixteen isolates were examined using PCR to determine whether they contained 16S rRNA or not. All of the isolates were positive (100%) for 16S rRNA, as shown in Fig. 1. The current findings

coincide with those of ^{24,25,26}; however, a different study by ²⁷ showed 96% susceptibility. Medical microbiology currently frequently uses 16S rRNA gene sequencing as a rapid and low-cost substitute for phenotypic methods for bacterial identification ²⁸.

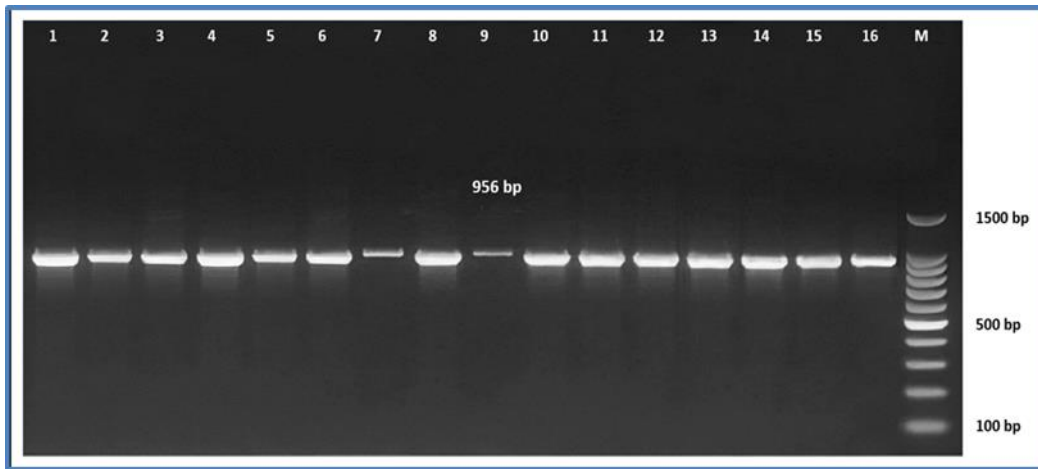


Figure 1. Results of *16srRNA* gene replication in clinical isolates of *P. aeruginosa*. Electrophoresed on 1.5 % agarose for 1 hour at 70 volts.

Antibiotics susceptibility test

Based on the Kirby-Bauer method test for antibiotic susceptibility, the isolates with the highest levels of resistance were Imipenem 12 (75%), Piperacillin 11 (68.75%), Gentamicin 10 (62.5%), Levofloxacin and Aztreonam 9 (56.25%), Meropenem and ceftazidime 8 (50%), Ciprofloxacin, Amikacin and

Piperacillin/ Tazobactam 7 (43.7%) and Ticarcillin/Clavulanate 6 (37.5%) (Fig. 2). Seven isolates (43.75%) were predicted to be multidrug-resistant (MDR) based on the CDC's classification of MDR, which is defined as an isolate that is resistant to at least one antibiotic in three or more medication classes.

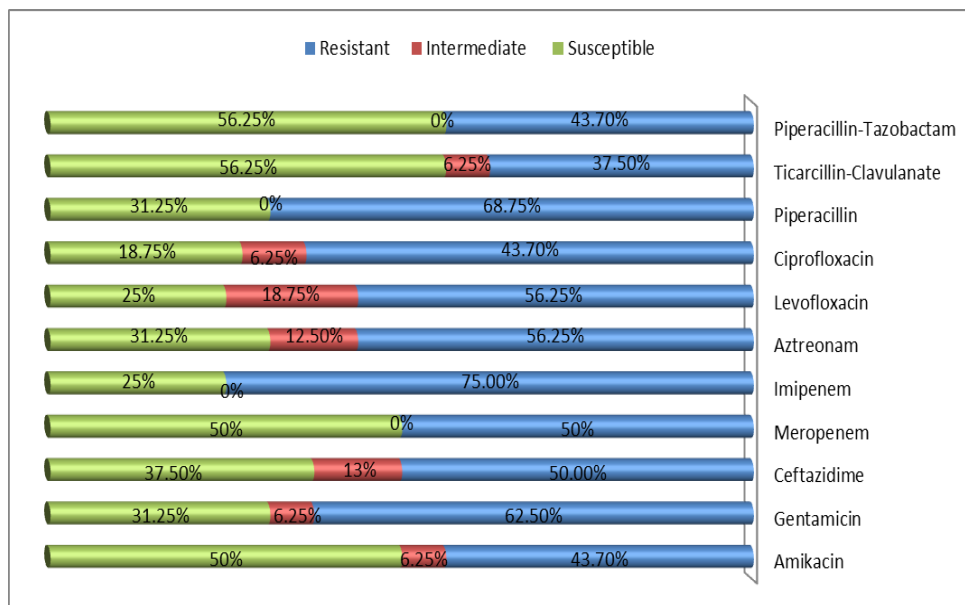


Figure 2. Percentage of Susceptibility of *P. aeruginosa* isolates to 11 antibiotics.

MDR-*P. aeruginosa* isolates were evaluated as 43.75% (n=7) at the time of the current study. According to research by ^{29,30}, 30.2% of the isolates were screened as MDR isolates. Other scientists discovered that 45.3%, 30.1%, and 5.46% of the isolates were also MDR. In a burn unit, resistant

infections are largely the cause of death. *P. aeruginosa* is one of the bacteria that primarily cause burn infections, although it also shows notable antibiotic resistance. Because of its poor permeability outer membrane, *P. aeruginosa* exhibits intrinsic resistance to a variety of

antimicrobial drugs³¹. However, other mechanisms also contribute to their intrinsic resistance, such as the generation of antibiotic-inactivating enzymes and efflux pumps, which actively eject antibiotics from bacterial cells to lower drug concentrations and cause drug resistance^{32,33}. The frequent use of antibiotics is another factor contributing to the rise in multidrug resistance (MDR). This is caused by the transfer of mobile genetic elements carrying resistance genes, such as plasmids encoding β -lactamases, and can happen during antibiotic therapy. Mutations in these elements can result in the overexpression of endogenous beta-lactamases or the expression of particular porins³².

PCR test results for efflux pumps genes detection

Four of the seven MDR bacterial isolates that tested positive for antibiotic resistance were chosen based on the findings of the antibiotic susceptibility test. Using a traditional uniplex PCR approach, the presence of efflux pump genes (*MexA*, *MexB*, *OprM*) and a housekeeping gene (*rpsL*) in four MDR *P. aeruginosa* isolates was examined. The findings revealed that every gene (100%) was present in the isolates that were tested (Fig. 3).

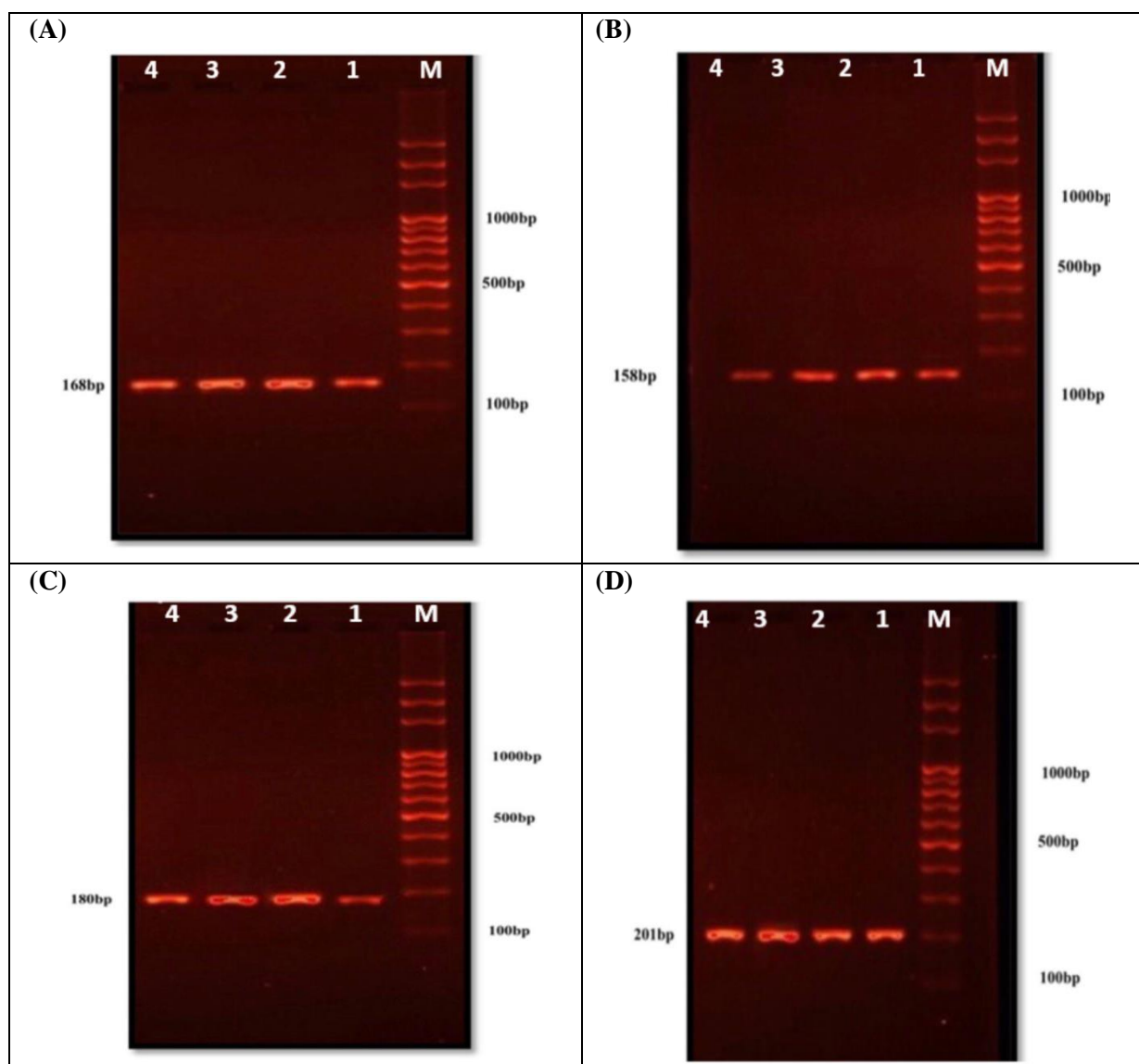


Figure 3. Agarose Gel electrophoresis of amplified PCR product for detection: A) *MexA* (168bp), B) *MexB* (158bp), C) *OprM* (180bp), and *rpsL* (201bp) gene run on 2% agarose for 60 min at 70 volts, stained with ethidium bromide, lane 1-4 *P. aeruginosa* isolates; M: DNA ladder.

Before examining gene expression, the present study assessed the existence of *MexAB-OprM* genes in *P. aeruginosa*. The findings showed that the efflux pump genes were present in all MDR isolates, which was consistent with the findings of ^{26,34-36} that concluded that *MexAB-OprM* genes existed in 100% of *P. aeruginosa* isolates. Furthermore, *MexAB-OprM* of *P. aeruginosa* was found in 100% of samples for both the *MexA* and *MexB* operon genes, according to ³⁷, demonstrating the chromosomal location of the *MexAB-OprM* efflux pump genes.

However, compared to earlier studies by ^{38,39}, which found the presence of the *MexA* and *MexB* genes in 58.8% and 70.58% of the isolates examined, respectively, the current study's percentage of both genes was higher than in the above-mentioned studies. While the results published by ⁴⁰ agreed with the current study that authorized isolates carried the *MexB* gene 100% of the time, another study conducted in Iran found that the *MexB* gene existed in 53.3% of isolates ⁴¹. These days, it is acknowledged that the efflux pump is one of the key complexes implicated in resistance to the majority of antibiotic classes ⁴².

Characterization of *Vitex* extract and ZnO NPs

In this research, the development of *Vitex* -ZnO NPs was characterized by a color shift from yellow to brown. After the ZnO salt was fully bio-reduced to ZnO NPs, the solution's color changed for a few hours. Zinc ions are transformed into ZnO NPs by flavonoids and phenolic substances. Phytochemicals can function as both reducing and stabilizing agents

because they are non-toxic compounds and antioxidants ⁴³. These findings were in line with the research by ^{44,45} that reported color variations in plant-mediated green production of ZnO NPs. After GC-MS analysis of the leaf extract components, it was found that the methanolic extract contained a high concentration of phytochemical components (> 50 chemical compounds) with anti-inflammatory and antibacterial properties, including Phytol (C₂₀H₄₀O), Phenol (C₆H₅OH), Vitamin E (C₂₉H₅₀O₂), 4,5-Dichloro-1,3-dioxolan-2-one (C₃H₂Cl₂O₃), Squalene (C₃₀H₅₀), and 4H-Pyran-4-one, 2,3-dihydro-3,5-dihydroxy (C₆H₈O₄). These conclusions are consistent with earlier research by ^{46,47}, which confirmed that the alcoholic extract included 36 and 93 chemical components, respectively, indicating that the *V. agnus* extract possesses a broad spectrum of chemical compounds. These substances fall under several chemical classes, such as flavonoids, glycosides, diterpenoids, essential oils, and phenolic compounds. Variations in the genotypes of *V. agnus* may be the cause of the variance in the number of phytochemical substances ⁴⁸.

The ZnO NPs' XRD patterns are displayed in Fig. 4. The peak locations of the X-ray diffraction are 31.8°, 34.4°, 36.3°, 47.5°, 56.6°, 62.8°, 66.4°, 67.9°, 69.1°, 72.5°, and 76.9°. As reflections, the XRD peaks were identified as (100), (002), (101), (102), (110), (103), (200), (112), (201), (004), and (202). The biosynthesized ZnO NPs' XRD patterns closely matched the earlier finding made by ⁴⁹.

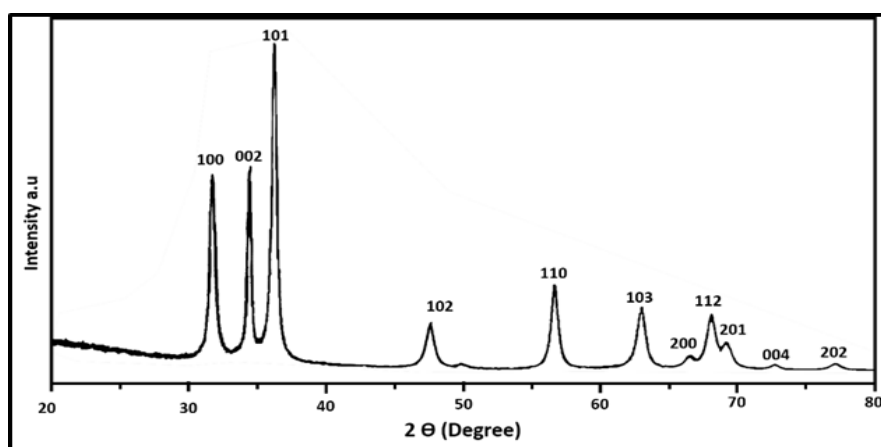


Figure 4. The XRD patterns of ZnO NPs.

In Fig. 5, the scanning electron microscopy (SEM) pictures depict the size and shape of ZnO NP. The particle size was between 22 and 74 nm, with a spherical and compact form. These findings are consistent with those of ⁵⁰, who also observed a

spherical morphology. In contrast, a different study's synthesis of ZnO nanoparticles using plant extract produced particles that were 40–50 nm in size and had a spherical morphology ⁵¹.

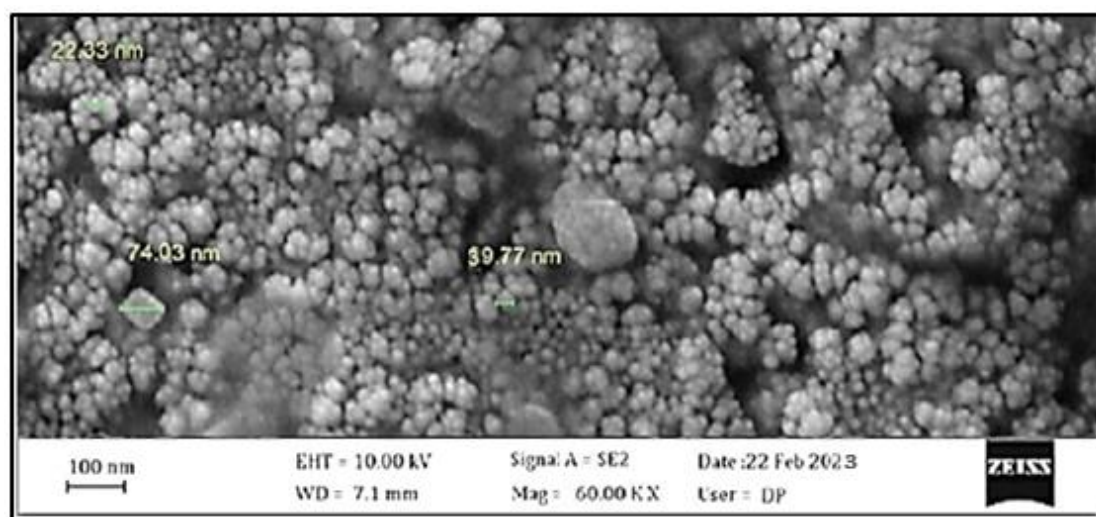


Figure 5. SEM image for ZnO-NPs synthesized

Antibacterial activity study and MIC determination ZnO NPs generated chemically had an antibacterial activity and MIC value of 1024 $\mu\text{g/ml}$ against MDR *P. aeruginosa*, while ZnO NPs biosynthesized using *V. agnus* leaf extract had a MIC value of 256 $\mu\text{g/ml}$ and a MIC value of 512 $\mu\text{g/ml}$. ZnO-NP has been proven to exhibit antibacterial action in a few earlier experiments. Regarding biosynthesized ZnO-NP, ^{12,52} found that the MIC values varied between 1600–3200 $\mu\text{g/ml}$ and 150 $\mu\text{g/ml}$ against isolates of *P. aeruginosa* that were resistant to multiple drugs, respectively. Disparities in ZnO nanoparticle manufacturing techniques and particle sizes could be the cause of variable findings regarding the toxicity of these particles. After researching ZnO-NP with a size of 30–90 nm against *P. aeruginosa* ⁵³, revealed that the MIC was 300 $\mu\text{g/ml}$. According to ⁵⁴, ZnO nanoparticles smaller than 20 nm have a stronger antigrowth effect than larger ones; this may be because they can more easily pass through the bacterial cell wall. Zinc oxide nanoparticles are generally antimicrobial; they can prevent bacteria from growing by penetrating the cell membrane; additionally, they can lead to oxidative stress, which can harm proteins, carbohydrates, lipids, and DNA ⁵⁵. The high negative charge on the cell surface of

gram-negative bacteria compared to gram-positive bacteria is another mechanism that could explain the increased antibacterial activity of ZnO-NP. As a result, gram-negative bacteria support the oxidative stress mechanism involved in zinc oxide nanoparticle antibacterial activity ⁵⁶ When compared to chemically produced ZnO NPs, the results of antibacterial activity indicate that the biosynthesized ZnO NPs have higher inhibitory action. According to ⁵⁷, chemical synthesis may potentially even now result in the presence of some harmful chemical species adsorbed on the surface that could have negative consequences in healthcare applications. As a result, the Bio-ZnO NPs enter the bacteria and attach themselves to the cell membrane with great ease.

The minimum inhibitory concentration (MIC) of *V. agnus* extract against multidrug-resistant *P. aeruginosa* was 512 $\mu\text{g/ml}$. The *Vitex agnus-castus* plant is regarded as one of the significant medicinal plants that has drawn significant interest and investigation from scholars ⁵⁸. According to ⁵⁹, the capacity of the essential oil derived from *V. gardneriana* to influence microbial cells shown antibacterial efficacy against *P. aeruginosa*. The antibacterial properties of alcoholic *V. agnus-castus*

extract can be attributed to flavonoids, tannins, and phenols—active phytochemical compounds found in medicinal plants—or to the hydroxyl groups (-OH) found in phenols, which have the capacity to form hydrogen bonds with the water molecules in bacterial cells, disrupting the bacterial cell's essential functions. Furthermore, the ability of tannins to inactivate enzymes, microbial adhesions, cell membranes that prevent *P. aeruginosa* transport proteins from growing, and other mechanisms may be linked to their action⁵⁸. The specific mechanism by which ZnO-NPs kill bacteria can be understood in a variety of ways. For example, their unique inhibitory mechanisms may stem from their capacity to produce toxic ions (Zn^{2+}), which compromise the integrity of the bacterial cell wall. Once inside the cells, the NPs and free metal ions disrupt biochemical processes by inducing denaturation of proteins and DNA damage⁶⁰. When the bacteria inside the microbial cells are unable to multiply regularly, this will ultimately result in cell

death and high amounts of reactive oxygen species (ROS)⁶¹.

Effects of ZnO -NPs and *V. agnus* extract on efflux pump Gene expression

Every bacterial isolate's total RNA was successfully extracted both before and after treatment with. The folding ($2^{-\Delta Ct}$) method was employed to quantify the gene expression levels, and the ΔCt value was adjusted to correspond with the housekeeping gene (*rpsL*). Tables 4, 5, 6 demonstrate that the expression of the *MexA*, *MexB*, and *OprM* genes was lower (fold expression <1) in the treated group isolates than in the untreated control group (fold expression =1). Cycle threshold, or Ct value, was used to measure the amplification; low Ct values indicate high expression, and high Ct values indicate reduced expression of the gene (Fig. 6). The quantitatively investigated using melting curve analysis and amplification plot (Fig. 7).

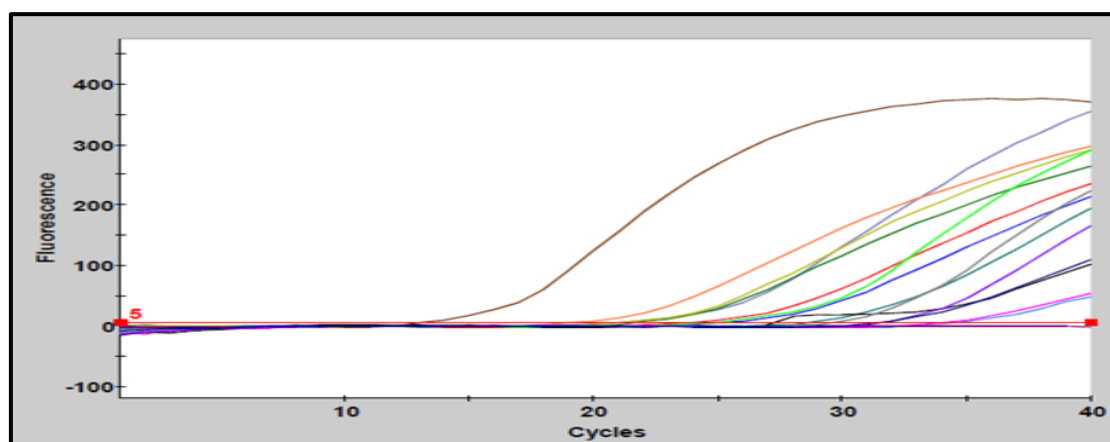


Figure 6. Results of *MexA* gene amplification curve by cycle in RT-PCR.

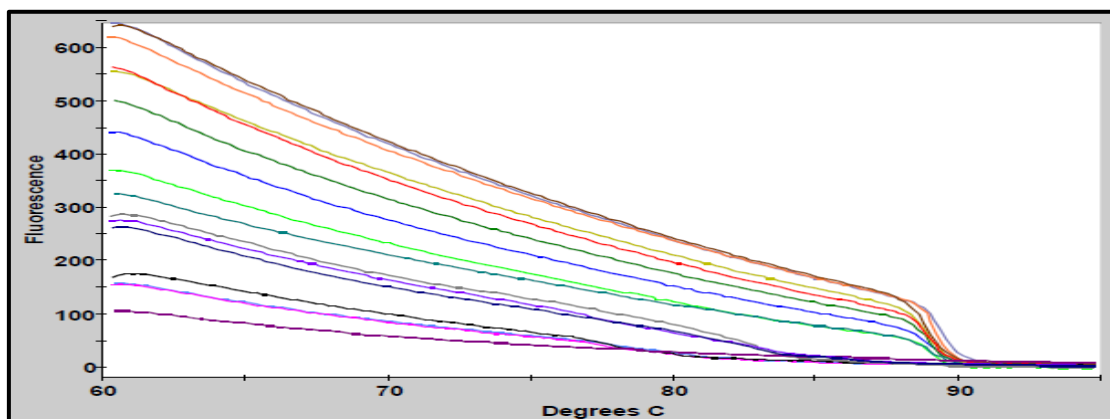


Figure 7. Melting curve analysis of the *MexA* gene. The measured curves of the gene in all samples are consistent and in the form of single-dot

The overexpression of the efflux pump genes (*MexA*, *MexB*, *OprM*) in the untreated *P. aeruginosa* isolates (= 1) was found to be associated with resistance mechanisms in MDR *P. aeruginosa*, as confirmed by the results of biosynthesized ZnO-NPs, chemically synthesized ZnO-NPs, and *V. agnus* extract. Additionally, *MexAB-OprM* appears to be very helpful during antibiotic pressure in the medical environment and may be vital for the efflux of many drugs of a direct association between antibiotic resistance and the expression of the *MexA* and *MexB* genes was in line with our results ⁶². The results displayed in (Fig. 8) indicate that biosynthesized ZnO-NPs has a stronger inhibitory effect on efflux pump genes than chemically synthesized ZnO-NPs and *V. agnus* extract, respectively. The expression of all the efflux pumps' genes was dramatically downregulated, except for *OprM*, where the effect of chemically synthesized ZnO-NPs was greater than that of *V. agnus* extract,

and *MexB*, where the effects of both biosynthesized ZnO-NPs and *V. agnus* extract were similar.

Since they can change the DNA strand and gene expression, ZnO -NPs and *Vitex* extract appear to affect the efflux pump genes of bacteria by increasing the formation of reactive oxygen species (ROS). Furthermore, RNA is extremely vulnerable to oxidative damage brought on by ROS, in contrast to DNA. By blocking MDR efflux pumps, nanoparticles could improve the effectiveness of conventional antibiotics as a treatment. Conversely, the existence of significant bioactive compounds may be responsible for the inhibitory activity of VA-C extracts ⁶³; some of these compounds may inhibit or lessen the formation of germ tubes (Pseudohyphae), adhesions, enzyme production, biofilm formation, and quorum sensing, among other virulence factors ⁶⁴.

Table 4. Comparison of *MexA* gene fold change between groups.

Material name	Group	Means CT of <i>MexA</i> gene	Means CT of HK gene	ΔCt	$2^{-\Delta Ct}$	Experimental group /control group	Fold change
Biosynthesized ZnO-NPs	Group1 (control)	21.06	18.84	2.22	0.2146	0.2146/0.2146	1.00 ±0.00
	Group2 (After treatment)	31.74	18.69	13.05	0.0001	0.0001/0.2146	0.0004 ±0.0001
T-test (P-value)		--	--	--	--	--	0.439 * (0.0467)
Chem.synthesized ZnO-NPs	Group1 (control)	21.06	18.84	2.22	0.2146	0.2146/0.2146	1.00 ±0.00
	Group2 (After treatment)	23.82	18.81	5.01	0.0310	0.0310/0.2146	0.1444 ±0.05
T-test (P-value)		--	--	--	--	--	0.502 * (0.0492)
<i>Vitex</i> extract	Group1 (control)	21.06	18.84	2.22	0.2146	0.2146/0.2146	1.00 ±0.00
	Group2 (After treatment)	24.77	18.66	6.11	0.0144	0.0144/0.2146	0.0671 ±0.019
T-test (P-value)		--	--	--	--	--	0.488 * (0.0431)

* (P≤0.05).

Table 5. Comparison of *MexB* gene fold change between groups.

Material name	Group	Means CT of <i>MexB</i> gene	Means CT of HK gene	ΔCt	$2^{-\Delta Ct}$	Experimental group /control group	Fold change
Biosynthesized ZnO-NPs	Group1 (control)	18.27	18.84	-0.57	1.484	1.484/1.484	1.00 \pm 0.00
	Group2(After treatment)	27.4	18.69	8.71	0.0023	0.0023/1.484	0.0015 \pm 0.0002
	T-test (P-value)	--	--	--	--	--	0.511 * (0.0419)
Chem. synthesized ZnO-NPs	Group1 (control)	18.27	18.84	-0.57	1.484	1.484/1.484	1.00 \pm 0.00
	Group2 (After treatment)	21.25	18.81	2.44	0.1842	0.1842/1.484	0.1241 \pm 0.04
	T-test (P-value)	--	--	--	--	--	0.485 * (0.0422)
<i>Vitex</i> extract	Group1 (control)	18.27	18.84	-0.57	1.484	1.484/1.484	1.00 \pm 0.00
	Group2 (After treatment)	27.2	18.66	8.54	0.0026	0.0026/1.484	0.0018 \pm 0.0003
	T-test (P-value)	--	--	--	--	--	0.547 * (0.039)

* (P \leq 0.05).

Table 6. Comparison of *OprM* gene fold change between groups gene.

Material name	Group	Means CT of <i>OprM</i> gene	Means CT of HK gene	ΔCt	$2^{-\Delta Ct}$	Experimental group /control group	Fold change
Biosynthesized ZnO-NPs	Group1 (control)	17.86	18.84	-0.98	1.972	1.972/1.972	1.00 \pm 0.00
	Group2 (After treatment)	31.89	18.69	13.2	0.0001	0.0001/1.972	0.0005 \pm 0.0002
	T-test (P-value)	--	--	--	--	--	0.532 * (0.045)
Chem. synthesized ZnO-NPs	Group1 (control)	17.86	18.84	-0.98	1.972	1.972/1.972	1.00 \pm 0.00
	Group2 (After treatment)	22.48	18.97	3.65	0.079	0.1593/1.972	0.0400 \pm 0.01
	T-test (P-value)	--	--	--	--	--	0.439 * (0.0382)
<i>Vitex</i> extract	Group1 (control)	17.86	18.84	-0.98	1.972	1.972/1.972	1.00 \pm 0.00
	Group2 (After treatment)	20.65	18.66	1.99	0.2517	0.2517/1.972	0.1270 \pm 0.03
	T-test (P-value)	--	--	--	--	--	0.537 * (0.0455)

* (P \leq 0.05).

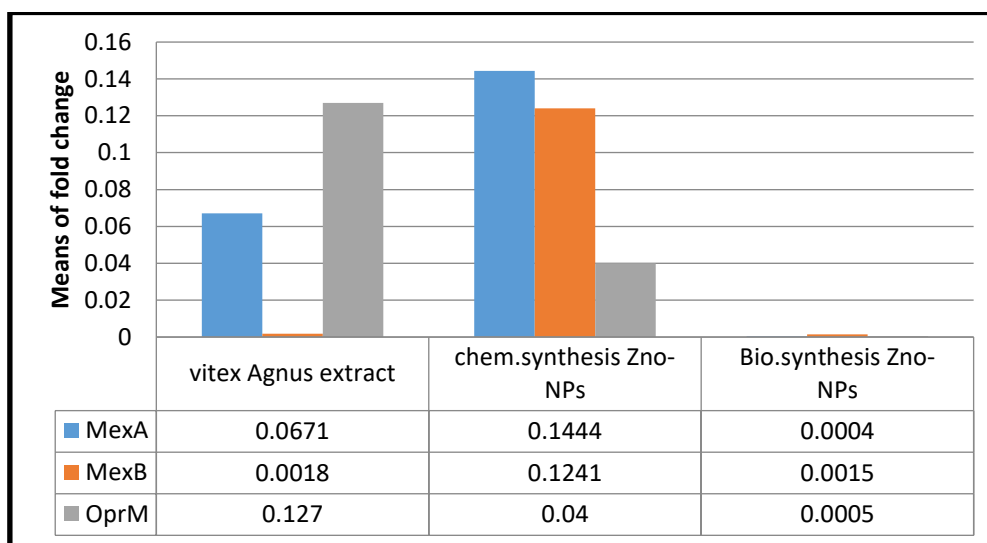


Figure 8. The expression rates of efflux pump genes in the biosynthesized ZnO –NPs, chemically synthesized ZnO –NPs and *V. agnus* extract -treated isolates and a significant decrease in gene expression was observed.

Conclusion

One of the primary causes of *P. aeruginosa* resistance is the *MexAB-OprM* system. A decrease in the level of these efflux pumps reduces the excretion of antibiotics from the cell, which in turn causes lower concentrations of antibiotics to be able to kill cells. The present investigation's results

showed that biosynthesized ZnO-nanoparticles using *V. agnus* extract reduced the number of active efflux pumps by reducing the expression of *MexA*, *MexB*, and *OprM* genes more than *V. agnus* extract alone and chemically synthesized ZnO-NP respectively.

Acknowledgment

Authors would like to express their deep gratitude to everyone who contributed in this study. Prof. Dr. Asmaa M. Salih Almohaidi who designed the

primers as well as to the staff of the ministry of science and technology especially Dr. Jwan Sabah Bajilan and Maha Mohammad.

Authors' Declaration

- Conflicts of Interest: None.
- We hereby confirm that all the Figures and Tables in the manuscript are ours. Furthermore, any Figures and images, that are not ours, have been included with the necessary permission for re-publication, which is attached to the manuscript.
- No animal studies are present in the manuscript.

- No human studies are present in the manuscript.
- Authors sign on ethical consideration's approval (the Code number of health ministry approved 2779).
- Ethical Clearance: The project was approved by the local ethical committee in University of Baghdad.

Authors' Contribution Statement

This study was carried out with contribution of all authors. S.T.A. was the one who developed the theoretical idea of the project and fully supervised

on work and writing with publishing while the practical part and writing the draft was the responsibility of S.A.K.K.

References

1. Shehab ZH, Ahmed ST, Abdallah NM. Genetic variation of pilB gene in *Pseudomonas aeruginosa* isolated from Iraqi patients with burn infections. *Ann Trop Med Public Health*. 2020 ; 23 (16) : 33-35. <http://doi.org/10.36295/ASRO.2020.231615>
2. Altaai ME, Aziz IH, Marhoon AA. Identification *Pseudomonas aeruginosa* by 16s rRNA gene for Differentiation from Other *Pseudomonas* Species that isolated from patients and environment. *Baghdad Sci J*. 2014 ; 11(2) : 1028-1034. <https://doi.org/10.21123/bsj.2014.11.2.1028-1034>
3. Papagiannitsis CC, Medvecky M, Chudejova K, Chudějová k, Skálová A , Rotova V, et al Molecular characterization of carbapenemase-producing *Pseudomonas aeruginosa* of Czech origin and evidence for clonal spread of extensively resistant sequence type 357 expressing IMP-7 metallo- β -lactamase. *Antimicrob Agents Chemother*. 2017 ; 61(12) :10-1128. <https://doi.org/10.1128/aac.01811-17>
4. Ahmed NA, Ahmed ST, Almohaidi AMS. Association of pvc genes expression with Biofilm formation in Clinical Isolates of *Pseudomonas aeruginosa*. *Baghdad Sci J*. 2024; 21(2): 261. <https://doi.org/10.21123/bsj.2023.7823>
5. Salumi Z, Abood Z. Phenotypic Diagnosis of Efflux Pump of *Escherichia coli* Isolated from Urinary Tract Infections. *Iraq J biotechnol*. 2022; 21(2) : 21-13.
6. Alibert S, N'gompaza Diarra J, Hernandez J, Stutzmann A, Fouad M, Boyer G, et al. Multidrug efflux pumps and their role in antibiotic and antiseptic resistance: a pharmacodynamic perspective. *Expert Opin Drug Metab Toxicol*. 2017 ; 13(3) : 301-309. <https://doi.org/10.1080/17425255.2017.1251581>.
7. Alcalde-Rico M, Hernando-Amado S, Blanco P, Martínez JL. Multidrug Efflux Pumps at the Crossroad between Antibiotic Resistance and Bacterial Virulence. *Front microbiol*. 2016; 7: 1483. <https://doi.org/10.3389/fmicb.2016.01483>
8. Al-Grawi IGA, Al-Absali AK, Kareem NH, Belal SA. Occurrence of MexAB-OprM efflux pump operon on septicemic *Pseudomonas aeruginosa* chromosome. *Iraqi Postgraduate Med J*. 2012; 11(1): 97-102.
9. Mba IE, Nweze EI. Nanoparticles as therapeutic options for treating multidrug-resistant bacteria: Research progress, challenges, and prospects. *World J Microbiol Biotechnol*. 2021 ; 37 : 1-30. <https://doi.org/10.1007/s11274-021-03070-x>
10. Hamrayev H, Shameli K, Korpayev S. Green synthesis of zinc oxide nanoparticles and its biomedical applications: A review. *Nanosci nanotechnol res*. 2021; 1(1): 62-74. <https://doi.org/10.37934/jmn.1.1.6274>
11. Naveed Ul Haq A, Nadhman A, Ullah I, Mustafa G, Yasinzai M, Khan I. Synthesis approaches of zinc oxide nanoparticles: the dilemma of ecotoxicity. *J Nanomater*. 2017 ; 2017: 14. <https://doi.org/10.1155/2017/8510342>
12. Ali SG, Ansari MA, Alzohairy MA, Alomary MN, Jalal M, AlYahya S, et al. Effect of biosynthesized ZnO nanoparticles on multi-drug resistant *Pseudomonas aeruginosa*. *Antibiotics*. 2020; 9(5) : 260. <https://doi.org/10.3390%2Fantibiotics9050260>
13. Qamar SUR, Ahmad JN. Nanoparticles: Mechanism of biosynthesis using plant extracts, bacteria, fungi, and their applications. *J Mol Liq*. 2021; 334 : 116040. <https://doi.org/10.1016/j.molliq.2021.116040>
14. Berrani A, Marmouzi I, Bouyahya A. Phenolic compound analysis and pharmacological screening of vitex agnus-castus functional parts. *Biomed Res Int*. 2021; 2021 : 1-10. <https://doi.org/10.1155/2021/6695311>
15. Dobrucka R. Facile synthesis of trimetallic nanoparticles Au/CuO/ZnO using Vitex agnus-castus extract and their activity in degradation of organic dyes. *Int J Environ Anal Chem*. 2021; 101 (14) : 2046-2057. <https://doi.org/10.1080/03067319.2019.1691543>
16. Crabbé A, De Boever P, Van Houdt R, Moors H, Mergeay M, Cornelis P. Use of the rotating wall vessel technology to study the effect of shear stress on growth behaviour of *Pseudomonas aeruginosa* PA01. *Environ Microbiol*. 2008; 10(8) : 2098-2110. <https://doi.org/10.1111/j.1462-2920.2008.01631.x>
17. Arabestani MR, Rajabpour M, Mashouf RY, Alikhani MY, Mousavi SM. Expression of efflux pump MexAB-OprM and OprD of *Pseudomonas aeruginosa* strains isolated from clinical samples using qRT-PCR. *Arch Iran Med*. 2015; 18(2) : 1. PMID: 25644798.
18. Spilker T, Coenye T, Vandamme P, LiPuma JJ. PCR-based assay for differentiation of *Pseudomonas aeruginosa* from other *Pseudomonas* species recovered from cystic fibrosis patients. *J Clin Microbiol*. 2004; 42(5) : 2074-2079. <https://doi.org/10.1128/jcm.42.5.2074-2079.2004>
19. Haleem AM , Hameed AH , Al-Majeed RA , Hussein NN , Hikmat RA , Queen BK. Anticancer, Antioxidant, Antimicrobial and Cytogenetic Effects of Ethanol Leaves Extract of *Carthamus tinctorius*. *IOP Conf Ser Earth Environ Sci*. 2023; 1262 (5):

052. <https://doi.org/10.1088/1755-1315/1262/5/052035>
20. Pillai AM, Sivasankarapillai VS, Rahdar A, Joseph J, Sadeghfar F, Anuf A R, et al. Green synthesis and characterization of zinc oxide nanoparticles with antibacterial and antifungal activity. *J Mol Struct.* 2020; 1211: 128107. <https://doi.org/10.1016/j.molstruc.2020.128107>
21. Osman DAM, Mustafa MA. Synthesis and characterization of zinc oxide nanoparticles using zinc acetate dihydrate and sodium hydroxide. *J Nanosci Nanoeng.* 2015; 1(4): 248-251.
22. Khodair ZT, Khadom AA, Jasim HA. Corrosion protection of mild steel in different aqueous media via epoxy/nanomaterial coating: preparation, characterization and mathematical views. *J Mater Res Technol.* 2019; 8 (1): 424-435. <https://doi.org/10.1016/j.jmrt.2018.03.003>
23. Zotta MD, Nevins MC, Hailstone RK, Lifshin E. The determination and application of the point spread function in the scanning electron microscope. *Microsc Microanal.* 2018; 24(4): 396-405. <https://doi.org/10.1017/S1431927618012412>
24. Teh YJ, Bahari Jambek A, Hashim U. A study of nano-biosensors and their output amplitude analysis algorithms. *J Med Eng Technol.* 2017; 41(1): 72-80. <https://doi.org/10.1080/03091902.2016.1223195>
25. Al-Tememe TM. Molecular detection and phylogenetic analysis of *Pseudomonas aeruginosa* isolated from some infected and healthy ruminants in Basrah, Iraq. *Arch Razi Inst.* 2022; 77(2) : 537. <https://doi.org/10.22092/ari.2022.357802.2099>
26. Abbas HA, El-Ganiny AM, Kamel HA. Phenotypic and genotypic detection of antibiotic resistance of *Pseudomonas aeruginosa* isolated from urinary tract infections. *Afr Health Sci.* 2018; 18(1): 11-21. <https://doi.org/10.4314%2Fahs.v18i1.3>
27. Al-Shimmmary SMH, Mohamed NS, Al-Qaysi SAS, Almohaidi AMS. Phylogeny analysis of *gyrB* gene and 16S rRNA genes of *Pseudomonas aeruginosa* isolated from Iraqi Patients. *Res J Pharm Technol.* 2021 ; 14(5) : 2517-2521. <http://dx.doi.org/10.52711/0974-360X.2021.00443>
28. Didelot X, Bowden R, Wilson DJ, Peto TEA, Crook DW. Transforming clinical microbiology with bacterial genome sequencing. *Nat Rev Genet.* 2012; 13(9) : 601-612. <https://doi.org/10.1038/nrg3226>
29. M Ebrahimpour, I Nikokar, Ghasemi Y, H Sedigh Ebrahim-Saraie, A Araghian, M Farahbakhsh, et al. Antibiotic resistance and frequency of class 1 integrons among *Pseudomonas aeruginosa*, isolated from burn patients in Guilan, Iran. *Iran J Microbiol.* 2013; 5(1): 36. <http://dx.doi.org/10.7416/ai.2018.2202>
30. Pérez A, Gato E, Pérez-Llarena J, Fernández-Cuenca F, Gude MJ, Oviaño M, et al. High incidence of MDR and XDR *Pseudomonas aeruginosa* isolates obtained from patients with ventilator-associated pneumonia in Greece, Italy and Spain as part of the MagicBullet clinical trial. *J Antimicrob Chemother.* 2019; 74(5) : 1244-1252. <https://doi.org/10.1093/jac/dkz030>
31. Martin-Loeches I, Deja M, Koulenti D, Dimopoulos G, Marsh B, Torres A, et al. Potentially resistant microorganisms in intubated patients with hospital-acquired pneumonia: the interaction of ecology, shock and risk factors. *Intensive Care Med.* 2013; 39: 672-681. <https://doi.org/10.1007/s00134-012-2808-5>
32. Adabi M, Talebi-Taher M, Arbabi L, Afshar M, Fathizadeh S, Minaeian S, et al. Spread of efflux pump overexpressing-mediated fluoroquinolone resistance and multidrug resistance in *Pseudomonas aeruginosa* by using an efflux pump inhibitor. *Infect Chemother.* 2015; 47(2): 98-104. <https://doi.org/10.3947/ic.2015.47.2.98>
33. Cunrath O, Meinel DM, Maturana P, Fanous J, Buyck JM, Saint Auguste P, et al. Quantitative contribution of efflux to multi-drug resistance of clinical *Escherichia coli* and *Pseudomonas aeruginosa* strains. *EBioMedicine.* 2019; 41: 479-487. <https://doi.org/10.1016/j.ebiom.2019.02.061>
34. Arabestani MR, Rajabpour M, Mashouf RY, Alikhani MY, Mousavi SM. Expression of efflux pump MexAB-OprM and OprD of *Pseudomonas aeruginosa* strains isolated from clinical samples using qRT-PCR. *Arch Iran Med.* 2015; 18(2): 1. <http://dx.doi.org/10.1016/j.genrep.2020.100744>
35. Rana T, Kaur N, Farooq U, Khan A, Singh S. Efflux as an arising cause of drug resistance in Punjab-India. *Int J Biol Pharm Allied Sci .* 2015; 4(9): 5967-5979. <https://doi.org/10.21474/ijar01/2971>
36. Dorri K, Modaresi F, Shakibaie MR, Moazamian E. Effect of gold nanoparticles on the expression of efflux pump *mexA* and *mexB* genes of *Pseudomonas aeruginosa* strains by Quantitative real-time PCR. *Pharmacia.* 2022; 69 (1): 125-133. <https://doi.org/10.3897/pharmacia.69.e77608>
37. Al-Grawi IGA, Al-Absali AK, Kareem NH, Belal SA. Occurrence of MexAB-OprM efflux pump operon on septicemic *Pseudomonas aeruginosa* chromosome. *Iraqi Postgraduate Med J.* 2012; 11(1): 97-102.
38. Kishk RM, Abdalla MO, Hashish AA, Nemr NA, El Nahhas N, Alkahtani S, et al. Efflux MexAB-mediated resistance in *P. aeruginosa* isolated from patients with healthcare associated infections. *Pathogens.* 2020; 9(6): 471. <https://doi.org/10.3390/pathogens9060471>

39. Bhandari S, Adhikari S, Karki D. Antibiotic resistance, biofilm formation and detection of mexA/mexB efflux-pump genes among clinical isolates of *Pseudomonas aeruginosa* in a Tertiary Care Hospital, Nepal. *Front. trop Dis.* 2022; 2: 810863. <https://doi.org/10.3389/fitd.2021.810863>
40. Al-Jumaily EF, Abd NQ. Effect of quinoline-2-one derivatives on the gene expression of mexB of *Pseudomonas aeruginosa*. *Biomed pharmacol J.* 2017 Sept 25; 10(3): 1475–9. <https://doi.org/10.13005/bpj/1255>
41. Pourakbari B, Yaslianifard S, Yaslianifard S, Mahmoudi S, Keshavarz-Valian S, Mamishi S. Evaluation of efflux pumps gene expression in resistant *Pseudomonas aeruginosa* isolates in an Iranian referral hospital. *Iran J Microbiol.* 2016; 8(4) : 249.
42. Shigemura K, Osawa K, Kato A. Association of overexpression of efflux pump genes with antibiotic resistance in *Pseudomonas aeruginosa* strains clinically isolated from urinary tract infection patients. *J Antibiot (Tokyo).* 2015; 68(9) : 568-572. <https://doi.org/10.1038/ja.2015.34>
43. Singh J, Dutta T, Kim KH, Rawat M, Samddar P, Kumar P. 'Green' synthesis of metals and their oxide nanoparticles: applications for environmental remediation. *J Nanobiotechnology.* 2018; 16(1) : 1-24. <https://doi.org/10.1186/s12951-018-0408-4>
44. Naseer M, Aslam U, Khalid B, Chen B. Green route to synthesize Zinc Oxide Nanoparticles using leaf extracts of *Cassia fistula* and *Melia azadarach* and their antibacterial potential. *Sci Rep.* 2020; 10(1): 9055. <https://doi.org/10.1038/s41598-020-65949-3>
45. Rajiv P, Rajeshwari S, Venckatesh R. Bio-Fabrication of zinc oxide nanoparticles using leaf extract of *Parthenium hysterophorus* L. and its size-dependent antifungal activity against plant fungal pathogens. *Spectrochim Acta A Mol Biomol Spectrosc.* 2013; 112: 384-387. <https://doi.org/10.1016/j.saa.2013.04.072>
46. Ababutain IM, Alghamdi AI. In vitro anticandidal activity and gas chromatography-mass spectrometry (GC-MS) screening of *Vitex agnus-castus* leaf extracts. *PeerJ.* 2021; 9 :e10561. <https://doi.org/10.7717/peerj.10561>
47. Keikha N, Shafaghat M, Mousavia SM, Moudi M, Keshavarzi F. Antifungal effects of ethanolic and aqueous extracts of *Vitex agnus-castus* against vaginal isolates of *Candida albicans*. *Curr Med Mycol.* 2018; 4(1): 1. <https://doi.org/10.18502/cmm.v4i1.26>
48. Karaguzel O, Girmen B. Morphological variations of chaste tree (*Vitex agnus-castus*) genotypes from southern Anatolia, Turkey. *N Z J Crop Hortic Sci.* 2009; 37(3): 253-261. <https://doi.org/10.1080/01140670909510271>
49. Cárdenas KA, Domínguez J, Palacios E, García L, Ramírez PA, Flores M. Synthesis and Characterization of ZnO Nanoparticles Obtained from the Extract of *Schinus Molle*. Springer; 2021: 569-575. https://doi.org/10.1007/978-3-030-65493-1_58
50. Sukri SNAM, Shameli K, Wong MMT, Teow SY, Chew J, Ismail NA. Cytotoxicity and antibacterial activities of plant-mediated synthesized zinc oxide (ZnO) nanoparticles using *Punica granatum* (pomegranate) fruit peels extract. *J Mol Struct.* 2019; 1189: 57-65. <https://doi.org/10.1016/j.molstruc.2019.04.026>
51. Gur T, Meydan I, Seckin H, Bekmezci M, Sen F. Green synthesis, characterization and bioactivity of biogenic zinc oxide nanoparticles. *Environ Res.* 2022; 204: 111897. <https://doi.org/10.1016/j.envres.2021.111897>
52. Hassani SM, Nakhaei, MM, Forghanifard MM. Inhibitory effect of zinc oxide nanoparticles on *Pseudomonas aeruginosa* biofilm formation. *Nanomed J* 2015; 2: 121-128. <https://doi.org/10.1186/s12941-023-00639-2>
53. Saadat M, Mohammadi SR, Eskandari M. Evaluation of antibacterial activity of ZnO and TiO₂ nanoparticles on planktonic and biofilm cells of *Pseudomonas aeruginosa*. *Biosci Biotechnol Res Asia.* 2013; 10(2): 629-635. <https://doi.org/10.13005/bbra/1174>
54. Ma H, Williams PL, Diamond SA. Ecotoxicity of manufactured ZnO nanoparticles—a review. *Environ pollut.* 2013; 172 : 76-85. <https://doi.org/10.1016/j.envpol.2012.08.011>
55. Kelly KA, Havrilla CM, Brady TC, Abramo KH, Levin ED. Oxidative stress in toxicology: established mammalian and emerging piscine model systems. *Environ Health Perspect.* 1998; 106(7): 375-384. <https://doi.org/10.1289/ehp.98106375>
56. Zhang L, Jiang Y, Ding Y, Povey M, York D. Investigation into the antibacterial behaviour of suspensions of ZnO nanoparticles (ZnO nanofluids). *J Nanoparticle Res.* 2007; 9: 479-489. <https://doi.org/10.1007/s11051-006-9150-1>
57. Adavallan K, Krishnakumar N. Mulberry leaf extract mediated synthesis of gold nanoparticles and its antibacterial activity against human pathogens. *ANSN.* 2014; 5(2): 025018. <https://doi.org/10.1088/2043-6262/5/2/025018>
58. Habbab A, Sekkoum K, Belboukhari N, Cheriti A, Y Aboul-Enein H. Essential oil chemical composition of *Vitex agnus-castus* L. from Southern-West Algeria and its antimicrobial activity. *Curr Bioact Compd.*

- 2016; 12(1): 51-60.
<https://doi.org/10.2174/1573407212666160330152633>
59. Parcelli J, Helena L, Alves M, Cardoso N, Carolina A, Martins M, et al. Chemical composition, antioxidant, antimicrobial and antibiofilm activities of *Vitex gardneriana* schauer leaves's essential oil. *Microb Pathog.* 2019; 135: 103608-8.
<https://doi.org/10.1016/j.micpath.2019.103608>
60. Khan ZUH, Sadiq HM, Shah NS, Khan A U, Muhammad N, Hassan S UI, et al. Greener synthesis of zinc oxide nanoparticles using *Trianthema portulacastrum* extract and evaluation of its photocatalytic and biological applications. *J Photochem Photobiol B.* 2019; 192: 147-157.
<https://doi.org/10.1016/j.jphotobiol.2019.01.013>
61. Wang L, Hu C, Shao L. The antimicrobial activity of nanoparticles: Present situation and prospects for the future. *Nanomed J.* 2017; 12: 1227-49.
<https://doi.org/10.2147/IJN.S121956>
62. Ahmed FY, Aly UF, Abd El-Baky RM, Waly NGFM. Effect of titanium dioxide nanoparticles on the expression of efflux pump and quorum-sensing genes in MDR *Pseudomonas aeruginosa* isolates. *Antibiotics.* 2021; 10(6): 625.
<https://doi.org/10.3390/antibiotics10060625>
63. Sahib AHA, Al-Shareefi E, Hameed IH. Detection of Bioactive Compounds of *Vitex agnus-castus* and *Citrus sinensis* Using Fourier-transform infrared spectroscopic profile and Evaluation of Its Antimicrobial Activity. *Indian J Public Health Res Dev.* 2019; 10(1): 954. <https://doi.org/10.5958/0976-5506.2019.00184.0>
64. Liu X, Ma Z, Zhang J, Yang L. Antifungal compounds against *Candida* infections from traditional Chinese medicine. *Biomed Res Int.* 2017; 2017: 1-12. <https://doi.org/10.1155/2017/4614183>

تأثير جسيمات أوكسيد الزنك (ZnO) المصنعة كيميائياً مقارنةً بجسيمات أوكسيد الزنك المصنعة حيويًا باستخدام مستخلص نبات *Vitex agnus* على تعبير جينات مضخة التدفق (MexAB-OprM) في بكتيريا الزائفة الزنجارية المتعددة المقاومة للمضادات

شمس الشموس خالص خميس، شذى ذنون احمد

قسم علوم الحياة، كلية العلوم للبنات، جامعة بغداد، بغداد، العراق.

الخلاصة

كان هدف الدراسة الحالية هو معرفة كيف تؤثر جسيمات اوكسيد الزنك النانوية المصنعة كيميائياً باستخدام طريقة sol-gel مقارنة بالجسيمات المخلفة حيويًا باستخدام مستخلص أوراق نبات *Vitex agnus-castus* على التعبير الجيني لجينات مضخة التدفق (MexAB-OprM) في عزلات بكتيريا الزائفة الزنجارية المتعددة المقاومة للادوية MDR. تم استخدام تفاعل البوليميراز المتسلسل PCR للتحري عن جين 16S rRNA في 16 عزلة من *P. aeruginosa*. كان اختبار 16S rRNA ايجابيا لجميع عزلات *P. aeruginosa* (100%)، وان 7 (43.75%) من العزلات كانت من نوع MDR. كما أشارت النتائج إلى أن عزلات MDR تحمل جينات OprM و MexA و MexB. تم فحص المواد الكيميائية النباتية في مستخلص نبات *V. agnus* باستخدام فحص تحليل GC-MS و اظهر الفحص لمستخلص *Vitex* عن وجود مركبات فعالة. و وكانت احجام جسيمات اوكسيد الزنك النانوية المصنعة تتراوح ما بين 22 و 74. بلغت قيم MIC لكل من جسيمات اوكسيد الزنك النانوية المصنعة كيميائياً والمخلفة حيويًا وكذلك مستخلص *Vitex* 1024 و 256 و 512 ميكروغرام / مل على التوالي عند اختبارها ضد عزلات MDR تم دراسة التعبير لجينات MexA و MexB و OprM المعاملة مع ZnO NPs ومستخلص نبات *Vitex* بواسطة تقنية RT-PCR. اظهرت جسيمات اوكسيد الزنك النانوية المخلفة حيويًا تأثير مثبط أكبر على التعبير الجيني لجينات MexA و MexB و OprM من الجسيمات النانوية المصنعة كيميائياً ومستخلص نبات *V. agnus* في العينات المعاملة بالتركيز المثبط الأدنى لكل من جسيمات اوكسيد الزنك النانوية والمستخلص النباتي مقارنة بالعينات غير المعاملة. إحدى الطرق التي تعمل بها الجسيمات النانوية ضد البكتيريا هي قمع التعبير عن جينات مضخة التدفق، مما يقلل من عدد مضخات التدفق النشطة على سطح الخلية ونتيجة لذلك، يعتبر ZnO-NPs من قطاع الأدوية خياراً طبيياً محتملاً..

الكلمات المفتاحية: الزائفة الزنجارية، جزيئات أوكسيد الزنك النانوية، *Vitex*، MexA، MexB، OprM.